Acta Scientiarum

http://www.uem.br/acta
ISSN printed: 1806-2563
ISSN on-line: 1807-8664
Doi: 10.4025/actascitechnol.v36i2.19285

Locking beam influence on behavior of reinforced concrete two pile caps with embedded socket

Rodrigo Barros[1*] and José Samuel Giongo[2]

*[1]Escola de Ciências e Tecnologia, Universidade Federal do Rio Grande do Norte, Avenida Senador Salgado Filho, 3000, 59078-97, Lagoa Nova, Natal, Rio Grande do Norte, Brazil. [2]Departamento de Engenharia de Estruturas, Escola de Engenharia de São Carlos, Universidade de São Paulo, São Carlos, São Paulo, Brazil. *Author for correspondence. E-mail: rodrigobarros@ect.ufrn.br*

ABSTRACT. This paper analyzes the behavior of reinforced concrete two pile caps with embedded socket, used as connection in precast concrete structures. To this end, it was specifically studied the effect of the locking beam on the pile caps when supported by the lateral walls of the socket. A three-dimensional numerical analysis was developed using a software based on the finite element method (FEM), which considered the nonlinear physical behavior of the materials. It was found that for strut angle inclination close to 45º, the pile caps showed the same behavior, independent of the wall interfaces. The results indicated that the presence of a locking beam has no significant influence on the pile caps behavior and that the socket wall is able to effectively transfer the force from the beam to the piles.

Keywords: pile caps, reinforced concrete, embedded socket foundation, locking beam, computational modeling.

Influência da viga de travamento em blocos de concreto armado sobre duas estacas com cálice embutido

RESUMO. O trabalho analisa o comportamento de blocos de concreto Armado sobre duas estacas com cálice embutido, utilizado em ligações com pilares pré-moldados. Particularmente, verifica-se o efeito da viga de travamento no bloco, quando apoiada nas paredes laterais do cálice. Foi desenvolvia análise numérica tridimensional utilizando um programa baseado no método dos elementos finitos, no qual foi considerado o efeito da não linearidade física dos materiais. Constatou-se que para ângulos de inclinação da escora próximos a 45°, o bloco apresenta o mesmo comportamento na presença da viga, independente da conformação das paredes do cálice. Os resultados indicam que a presença da viga de travamento não altera de modo significativo o comportamento estrutural do bloco, e que as paredes do cálice são capazes de transferir de modo efetivo a força oriunda da viga de travamento para as estacas.

Palavras-chave: blocos sobre estacas, concreto armado, cálice embutido, viga de travamento, modelagem computacional.

Introduction

The emergence of new technologies and advances in the civil construction industry directly affects the construction process, regarding construction time, productivity increase and waste reduction. In this context, the use of precast concrete becomes widespread in the technical environment to meet these new requirements.

Precast elements are produced prior to their installation in the final structure, and have many transitory phases, like a demolding, storage, transport and assembly. As the structure has separate parts, it is necessary to use special elements for the connection between precast elements. Pile-caps are important parts for the connection between the precast column and foundations. One way to connect these elements is by using pile caps with sockets, which are widely used due to their construction facility, fit possibilities and transmission of moments from column to piles.

The socket is a part of the pile cap that receives the precast column, working as a joint between the elements, and the socket walls may have a smooth or rough interface. The column is in contact with the socket in a depth length, ℓ_{emb}. In this kind of connection, there are three possible situations for the socket: external, embedded and partially embedded.

The frequent use of precast elements in current structures requires from engineers technical and practical knowledge on the subject. In this context, there is still a wide gap to be filled with research and experiments. Some researchers such as Souza et al. (2007) and Nori and Tharval (2007) have developed studies on pile cap design using the Strut and Tie model. However, most studies consider

conventional concrete cast in situ, whose connection can be considered monolithic.

This paper presents a numerical simulation of reinforced concrete two pile caps with embedded socket. The locking beam influence on these elements is evaluated when positioned in the smaller direction of the pile caps. The analysis in this study consists of the results obtained from the numerical models using the software Diana 9.2., based on the Finite Method Elements. The physical nonlinearity of concrete and reinforcement bars was considered, as well as the rough or smooth interface of the column and socket.

The subject in study is relevant given the lack of research in the area. Souza et al. (2009) presents an adaptable Strut-and-Tie model for design and verification of four-pile caps. Experimental researches on pile caps with embedded socket are in development at the Structural Laboratory of Engineering School of São Carlos, based on numerical analysis.

The Strut-and-Tie model is based on classical truss analogy introduced in the early twentieth century by Mörsch and improved by Ritter, in which the cracked concrete beam is associated with a parallel chord truss. After years of studies, the model has evolved, resulting in the generalized Mörsch truss, in which the upper and lower flanges are not parallel near the restraints, the strut inclination is not constant and less than 45° throughout the beam. However, the basic idea of a beam associated with a classical truss remains valid.

The strut and tie model is a discrete representation of flow stress in a particular structural element. The initial structure is represented by an equivalent structure composed of compressed and tensioned bars connected by nodes. The compressed bars are called Struts and must absorb the compressive stress flow, usually represented by dashed lines. The tensile bars are called tie, and should absorb the tensile stress flow existing in the element, and represented by solid lines.

The strut-and-tie model will include struts, tie and nodes. In reinforced concrete elements, the strut represents concrete regions that are subjected to compression, while the tie represents the steel bars subjected to tension. Eventually, in some concrete structural elements the tie can be of concrete, once the maximum stress does not exceed the tensile strength of the material. There are multiple strut-and-tie models that satisfy equilibrium conditions. It should be considered that the structure tries to carry loads as effectively as possible with the least amount of deformation. Since the contribution of the tensile forces to displacement is much greater than that of concrete struts, a model with the shortest ties and least tie forces is the most effective.

Schlaich and Schäfer (1991) presents design and details of structural concrete using Strut-and-Tie models. Kwak and Noh (2006) presents structural optimization applied to Strut-and-Tie models. Further details for the Strut-and-Tie approaches and related theories for the design of structural concrete can be found in the state-of-the-art report by the ACI-ASCE Committee 445 (ASCE, 2009) on Shear design of structural concrete.

The locking beam is a structural element used between elements of the foundation, such as pile caps and footings, with the purpose of absorbing the construction eccentricity and settlements. In some situations, the locking beam can be used as a support element for ground floor masonry walls.

Material and methods

The numerical simulations were performed with the Finite Element Method using the software Diana 9.2, licensed to the Structural Engineering Department of Engineering School of São Carlos, University of São Paulo.

Two pile caps with embedded socket used in column-foundations connections were studied by computational modeling. The boundary conditions and the loads on pile caps reproduced an almost real project situation. Displacement on vertical direction was restricted on the pile. The mechanical properties of the materials used in the numerical models were obtained from standards ABNT (2007a and b) NBR 6118 and NBR 7480. For the constitutive model of concrete the strain softening was considered by the smeared crack model. The Total Strain with fixed crack model was used to represent the tension and compressive behavior of the material. For tension behavior it was adopted the exponential curve, and for compression behavior it was considered the parabolic curve, according Figure 1. The fracture energy G_f and the compressive fracture energy G_c were obtained by DIANA recommendations.

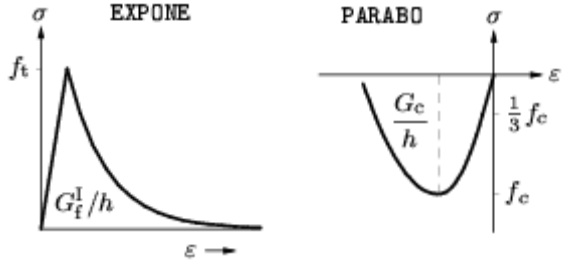

Figure 1. Predefined tensile and compressive behavior for Total Strain models. Diana (2005) material library.

The purpose of the numerical analysis is to evaluate two pile caps with embedded socket behavior, with regards to load versus displacement curves and principal flow stress. The numerical model presented on this paper was validated with experimental results of Delalibera and Giongo (2009).

The parameters chosen for the numerical simulations analysis were the following: The strut angle inclination; thickness of the lateral socket walls; the conformation of socket walls (smooth or rough); and the locking beam presence.

The strut inclination was equal to 45 and 55°. These values were chosen based on recommendations by Blévot and Frémy (1967), and obtained from equilibrium of forces. Two values were used for the lateral socket wall thickness: 0.15 m and 0.20 m. Due to the scarcity of information on embedded sockets, the recommendations by Leonhardt and Mönnig (1978) and standard ABNT (2006) NBR 9062 for external sockets were used. The conformation of the socket and walls were smooth or rough interfaces. For the locking beam, two different beam load values were used to verify its influence on the behavior of the pile caps. In total, 24 models of two pile caps with embedded socket separated into four groups were analyzed, presented in Tables 1 and 2.

To determine the action values of locking beam, two situations were considered. The first situation used a wall of concrete blocks, 0.14 x 0.19 x 0.29 m in size, and 5 m in height. The second situation used a wall of concrete blocks, 0.19 x 0.19 x 0.39 m in size, and 6 m in height. The first situation resulted in the action of 18.5 kN m^{-1}, called cv1. The second situation resulted in the action of 29.4 kN m^{-1}, called cv2.

The nomenclature used for the models was determined from the following parameters: conformation of socket walls, height of pile caps, strut inclination, thickness of lateral socket walls and load on the locking beam. Table 1 lists the nomenclature of models with smooth interface, and Table 2 shows the nomenclature of models with rough interface.

The geometry and characteristics of two pile cap models with embedded socket numerically analyzed by the software Diana 9.2 are presented. The two pile caps were designed as recommended by Blévot and Frémy (1967) for strut, and ABNT (2007a) NBR 6118 for reinforcement bars design. As the objective of the study is to analyze the behavior of pile caps with embedded socket in the presence of locking beams, the column geometry, piles and locking beam on the models were not changed.

As the models had centered load without moment, it was used 0.35 m value for ℓ_{emb} on pile caps with rough interface, disregarding the recommendation of minimum value of 0.40 m from ABNT (2006) NBR 9062. Table 3 presents the geometry and characteristics of the models analyzed in accordance with the groups previously presented.

Table 1. Nomenclature of numerically analyzed models with smooth interface.

Group	Model	Interface	Angle	Thickness (m)	Beam	Load
BLH75A45	BLH75A45_15	smooth	45º	0.15	without	-
	BLH75A45_15_cv1				With	cv1
	BLH75A45_15_cv2				with	cv2
	BLH75A45_20			0.20	without	-
	BLH75A45_20_cv1				with	cv1
	BLH75A45_20_cv2				with	cv2
BLH75A55	BLH75A55_15		55º	0.15	without	-
	BLH75A55_15_cv1				with	cv1
	BLH75A55_15_cv2				with	cv2
	BLH75A55_20			0.20	without	-
	BLH75A55_20_cv1				with	cv1
	BLH75A55_20_cv2				with	cv2

Table 2. Nomenclature of numerically analyzed models with rough interface.

Group	Model	Interface	Angle	Thickness (m)	Beam	Load
BRH65A45	BRH65A45_15	rough	45º	0.15	without	-
	BRH65A45_15_cv1				with	cv1
	BRH65A45_15_cv2				with	cv2
	BRH65A45_20			0.20	without	-
	BRH65A45_20_cv1				with	cv1
	BRH65A45_20_cv2				with	cv2
BRH65A55	BRH65A55_15		55º	0.15	without	-
	BRH65A55_15_cv1				with	cv1
	BRH65A55_15_cv2				with	cv2
	BRH65A55_20			0.20	without	-
	BRH65A55_20_cv1				with	cv1
	BRH65A55_20_cv2				with	cv2

Table 3. Geometry and characteristics of groups of models analyzed.

Groups	Pile Section (m^2)	Column Section (m^2)	Locking beam section (m^2)	B_{Lx} (m)	B_{Lv} (m)	ℓ_{emb} (m)	Height (m)
BLH75A45	0.30 x 0.30	0.30 x 0.30	0.20 x 0.40	2.05	0.70 / 0.80	0.45	0.75
BLH75A55	0.30 x 0.30	0.30 x 0.30	0.20 x 0.40	1.65	0.70 / 0.80	0.45	0.75
BRH65A45	0.30 x 0.30	0.30 x 0.30	0.20 x 0.40	1.85	0.70 / 0.80	0.35	0.65
BRH65A55	0.30 x 0.30	0.30 x 0.30	0.20 x 0.40	1.50	0.70 / 0.80	0.35	0.65

Note: B_{Lx} and B_{Ly} are pile caps length in x and y direction, respectively.

Columns and piles have squared section with 0.30 m sides. The lateral walls have two thickness values, 0.15 and 0.20 m. Furthermore, there is a 0.05 m gap between the column and socket, which is later filled with grout, resulting in B_{Ly} values.

The main reinforcement bar areas of tie were designed from the strut-and-tie model, while the column and pile had concrete with compressive characteristic strength greater than the compressive characteristic strength of pile caps. This procedure was made in order to prevent the collapse of the models in the column or piles. The yield stress used was equal to 500 MPa, while the elasticity module was equal to 210 GPa.

Figures 2a and b, 3a and b shows the reinforcement bars used on the pile caps studied, which are present on Table 4 for each group. Table 5 shows mechanical properties of concrete used in the models designed by ABNT (2007a) NBR 6118. In this case, f_{ck} is compressive characteristic strength, $f_{ct,m}$ is mean tension stress and E_{cs} is the secant elasticity modulus of concrete.

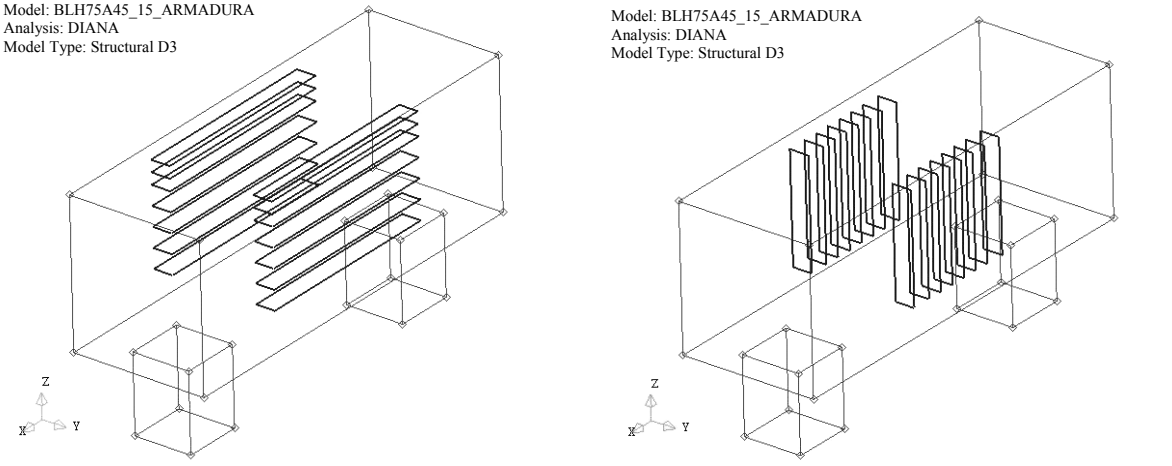

Figure 2. Reinforcement bars in socket walls.++

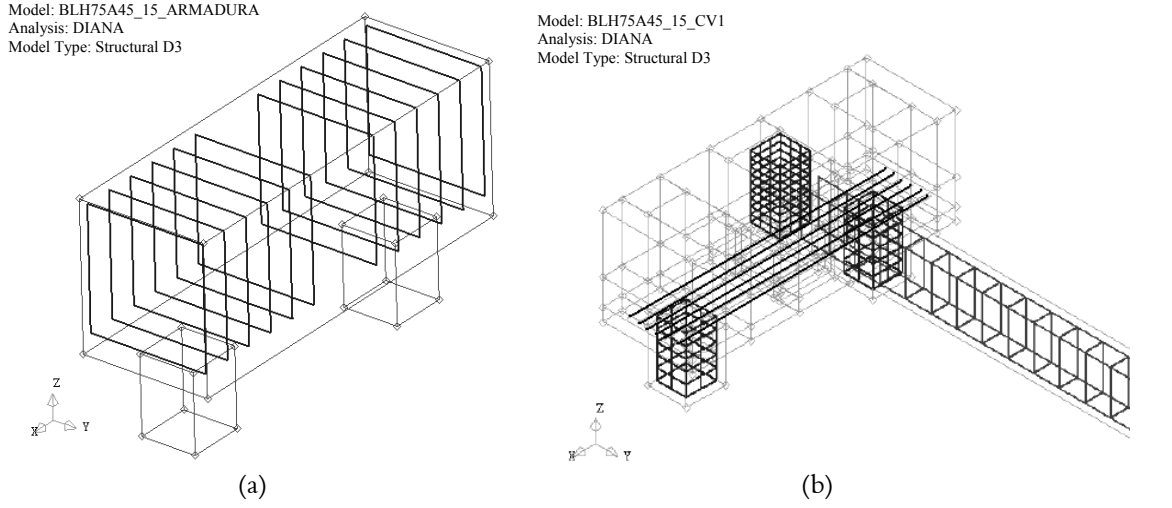

Figure 3. Reinforcement bars in pile caps and beam.

Table 4. Reinforcement bars of models.

Groups	BLH75A45	BLH75A55	BRH65A45	BRH65A55
Vertical Stirrups	6Ø6.3 c/10	6Ø6.3 c/11.5	6Ø6.3 c/13.5	6Ø6.3 c/15.5
Longitudinal bars	6Ø20 mm			
Horizontal Stirrups	4Ø6.3 c/15			
Column bars	12Ø12.5 mm			
Pile bars	8Ø12.5 mm			

Table 5. Concrete mechanical properties.

Properties	f_{ck} (MPa)	f_{ctm} (MPa)	E_{cs} (MPa)	G_F (N·mm mm^{-2})	G_c (N·mm mm^{-2})
Pile cap	25	2.56	23800	0.0692	3.45
Column	50	4.07	33658	0.1026	5.13
Pile	50	4.07	33658	0.1026	5.13
Beam	25	2.56	23800	0.0692	3.45
Grout	50	4.07	33658	0.1026	5.13

Note: values obtained in accordance with ABNT (2007a) NBR 6118 and Diana (2005).

The finite elements used in the numerical simulation were those available in the Diana (2005) element library. In this case, a solid element CHX60 was used for pile caps, column and piles. CHX60 is a twenty-node isoparametric solid brick element. It is based on quadratic interpolation and Gauss integration.

To simulate the reinforcement bar, an embedded reinforcement for Diana Library was used, which adds stiffness to the finite element model in contact with reinforcement. These elements are called mother elements and do not have their own degree of freedom. Reinforcement strains are computed from the displacement field of the mother elements. This implies perfect bond between the reinforcement and the surrounding material. Therefore, the adhesion between reinforcement bars and concrete is considered perfect.

To simulate a contact region between column - grout and grout – pile cap, interface elements based on friction model were used. The finite element used was a CQ48I, an interface element between two planes in a three-dimensional configuration, like a pile cap problem. This element was chosen because a connection with CHX60 element is necessary.

The use of interface elements was only performed on the pile caps with smooth interfaces. For rough walls, Canha et al. (2009) and Delalibera and Giongo (2009) found that, due the occurrence of shear key, it can be considered a monolithic connection.

According to Diana's manual, the interaction between two structural interfaces can be described as a friction behavior in these parts. The friction model of Coulomb presented in Diana and described by Chen (1982) shows this formulation. According to Chen (1982), usual friction angle values are around 37°. However, this value implies tensile stress around 25% of compression stress, values considered high for usual concretes. Therefore, a friction angle equal to 31° was adopted, whose tangent results in 0.6 and the tensile stress was obtained in agreement with recommendations of ABNT (2007a) NBR 6118. The cohesion value was calculated by Equation (1), where fc' is the concrete characteristic compressive strength.

$$c = \frac{f_c^{'} \cdot (1 - sen\phi)}{2 \cdot \cos\phi} \quad (1)$$

The constitutive model used for the concrete was Total Strain with the fixed crack model. This model used a shear retention coefficient of 0.99 and energy convergence criterion with 1% of tolerance. The pressure was applied on the top of the column and on the locking beam, and the Regular Newton-Raphson method was used to solve the non linear system. The fracture energy on tensile and compression was adopted from Diana (2005) material library. Additional information on concrete modeling can be found in Bangash (2001).

Results and discussion

Pile caps with rough interface, θ=45

Pile caps with rough interface and locking beam presence had the same behavior as the pile caps without locking beam, regarding the curve load versus displacement, measured in the middle of pile caps. The presence of the locking beam does not significantly change the behavior of pile caps, and the socket wall is able to effectively transfer the force from the beam to the pile caps.

Figure 4a shows load versus displacement curve of three pile caps with rough interfaces, 0.15 m thick walls and two load requests on the locking beam: BRH65A45_15, BRH65A45_15_cv1 and BRH65A45_15_cv2. Figure 4-b presents the load versus displacement from similar models, but 0.20 m thick walls. Comparing the results, for the same load on the locking beam, the pile caps with 0.15 m thick walls have ultimate load higher than the pile caps with 0.20 m thick walls, as observed in Figure 5a and b for cv_1 and cv_2 load case, respectively.

Pile caps with smooth interface, θ=45

Similar to the rough interface pile caps, the locking beam presence did not change significantly the behavior of pile caps with smooth interface with regards to the load versus displacement curve. Figure 6a shows load versus displacement curve of three pile caps with smooth interface, 0.15 m thick walls and two load requests on the locking beam:

BLH75A45_15, BLH75A45_15_cv1 and BLH75A45_15_cv2. Figure 6b presents the load versus displacement from similar models, but with 0.20 m thick walls.

Considering the thickness of walls, once again 0.15 m thick pile caps walls have an ultimate load higher than of the 0.20 m pile caps walls. The results are presented in Figure 7a and b for load case cv_1 and cv_2.

Pile caps with rough interface, θ=55

The situation of pile caps with rough interface and strut angle of 55° showed different results when compared to other models. These models presented an ultimate load lower than pile caps with strut angle equal to 45° with the presence of a locking beam. For the models with 0.15 m thick walls, they obtained a 7% reduction of ultimate load when compared to the model without locking beam. For the models with 0.20 m thick walls, the reduction was equal to 14%. However for the models with 0.20 m thick walls, the load versus displacement curve of the model BRH65A55_20 had an adaptation close to 2450 kN force and 1.2 mm displacement. The force was constant while the displacement increased to 1.5 mm, when the model again improves, reaching a 2800kN load.

Figure 8a shows the load versus displacement curve of models with 0.15 m thick walls and Figure 8b shows the 0.20 m walls. Comparing only models with locking beams, the models with 0.15 m thick walls had ultimate load higher than the models with 0.20 m thick walls, as verified in Figure 9a and b.

Pile caps with smooth interface, θ=55

The results of pile caps with smooth interface and strut angle equal to 55° were similar to the pile caps with smooth interface and strut angle of 45°. The models BLH75A55_15, BLH75A55_15_cv1 and BLH75A55_15_cv2, as well as the models BLH75A55_20, BLH75A55_20_cv1 and BLH75A55_20_cv2 presented the same tendency in the load *versus* displacement curve. In other words, the locking beam did not significantly change the behavior of the pile caps. These results are shown in Figure 10a and b.

With regard to the thickness of walls, once again the pile caps with 0.15 m thick walls had an ultimate load higher than the pile caps with 0.20 m tick walls. The results are presented in Figure 11a and b for load case cv_1 and cv_2.

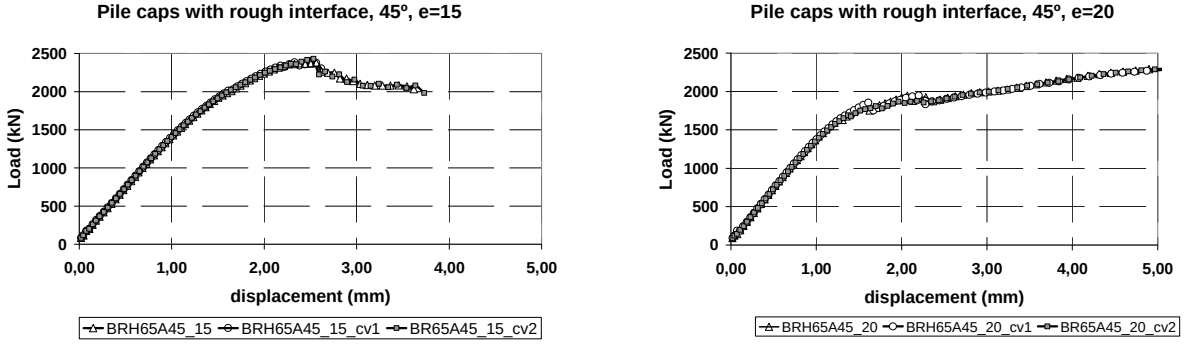

Figure 4. Locking beam influence on pile caps with rough interface, θ=45º.

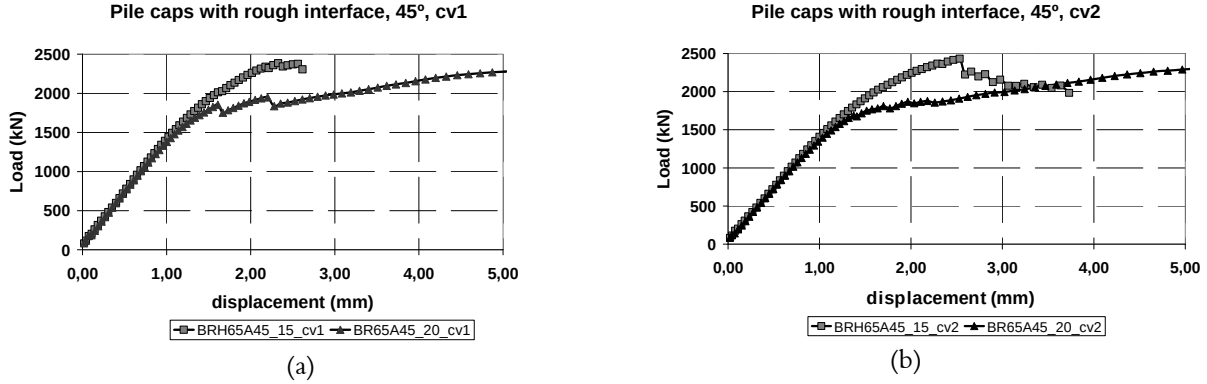

Figure 5. Load on locking beam influence on pile caps with rough interface, θ=45º.

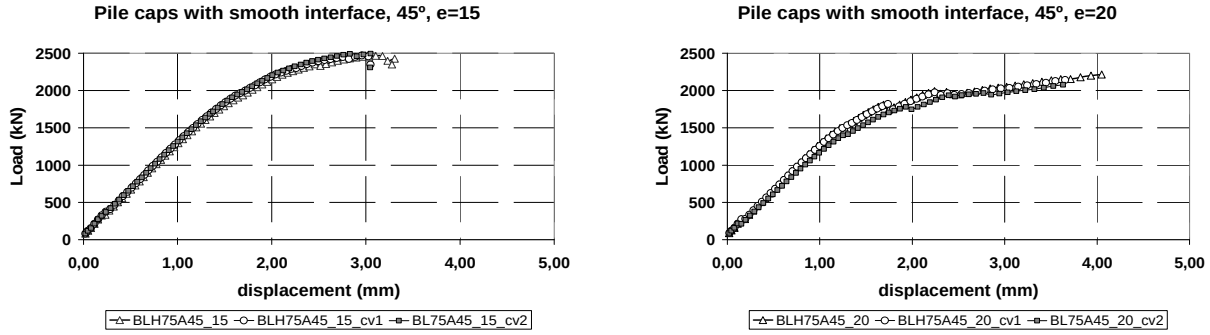

Figure 6. Locking beam influence on pile caps with smooth interface, θ=45º.

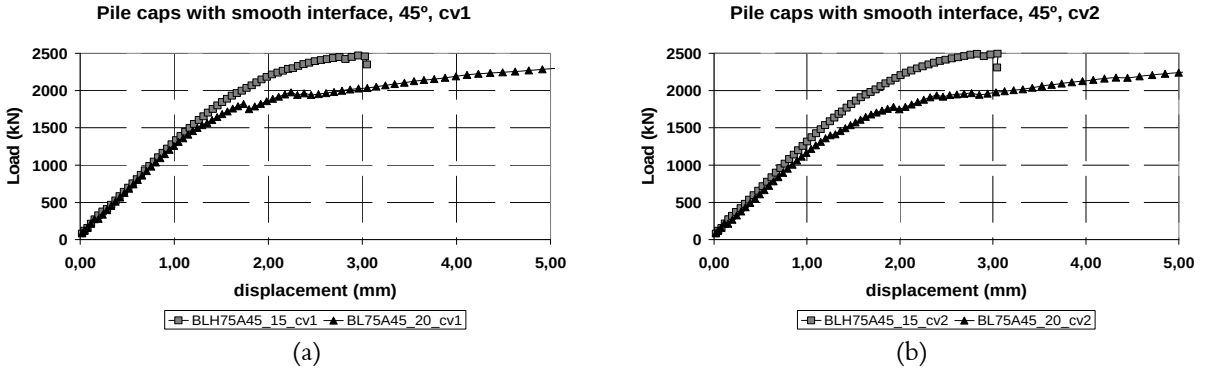

Figure 7. Load on locking beam influence on pile caps with smooth interface, θ=45º.

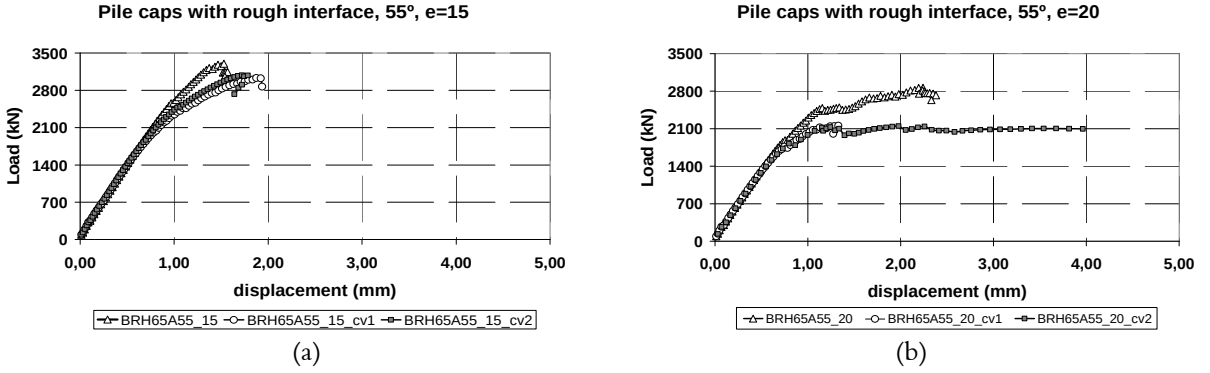

Figure 8. Locking beam influence on pile caps with rough interface, θ=55º.

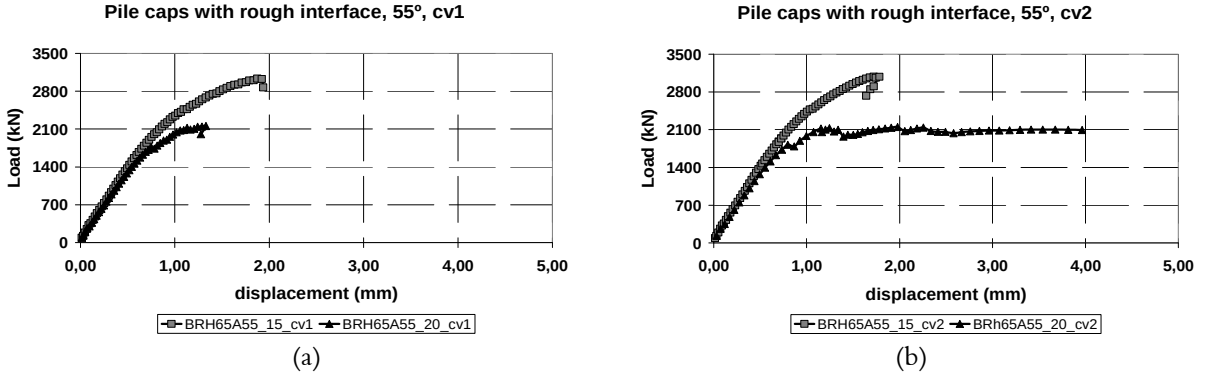

Figure 9. Load on locking beam influence on pile caps with rough interface, θ=55º.

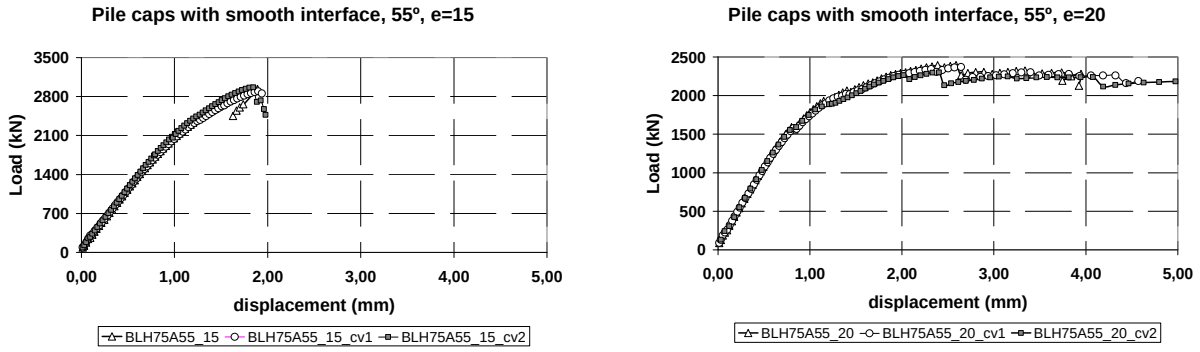

(a) (b)

Figure 10. Locking beam influence on pile caps with smooth interface, θ=55º.

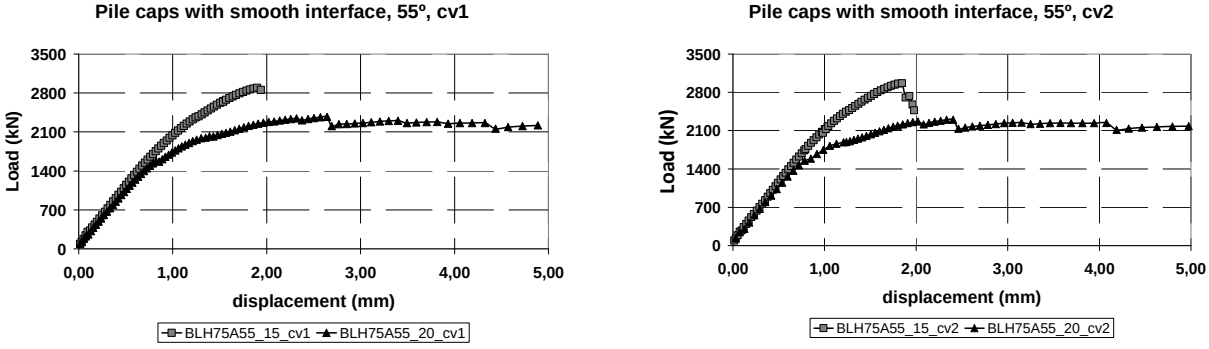

(a) (b)

Figure 11. Load on locking beam influence on pile caps with smooth interface, θ=55º.

In general, the failure mode of smooth models occurred on concrete of pile caps, without yield stress of main reinforcement bar. The pile caps with θ = 55º presented an ultimate load greater than models with θ = 45º, limited by compressive strength of concrete.

Due the number of models analyzed, are presented below the cracking panorama, compressive stress flow and principal stress flow of only one model. The Figure 12 shows a cracking panorama and Figure 13 shows the principal stress flow of the model BLH75A55_20.

The ultimate loads values in analyzed models are presented on Table 6, as well as the local collapse and the failure mode. The collapse in concrete occurred in models in which the reinforcement bar did not reach the yield stress, and the compressive stress value on pile caps was greater than compressive resistance of concrete. The pile caps with 0.15 m of lateral socket wall thickness presented fragile failure mode, without ductility after the ultimate load. The tensile stress on interface elements, existing only in models with smooth surface, presented values ranging from 0.7 to 1.3 MPa, lower than tensile resistance of concrete. This fact indicates that, for the pile caps studied herein, the ruin of models has not occurred in this region. Some models present normal stress higher than the yield stress. However, this is an isolated fact in a punctual part of the model.

For each group, models with 0.15 m wall thickness presented ultimate load greater than with 0.20 m wall thickness. To verify the influence of the socket wall, it was analyzed two other models with 0.25 m of wall thickness. The ultimate load of these models was lower than models with 0.15 and 0.20m, as illustrated in Figure 14.

According to models analyzed, the socket wall was able to effectively transfer the force from the beam to pile caps, without impairment of the behavior of pile caps. These results were different only for pile caps with rough interface and with strut angle of 55°, when it was observed a reduction in ultimate load value between 7 and 14%. However, these values are small to affirm that the decrease was caused by the presence of the locking beam. Regarding load values on the locking beam, the two values considered in the analysis do not change the pile cap behavior, showing the same load versus displacement curve.

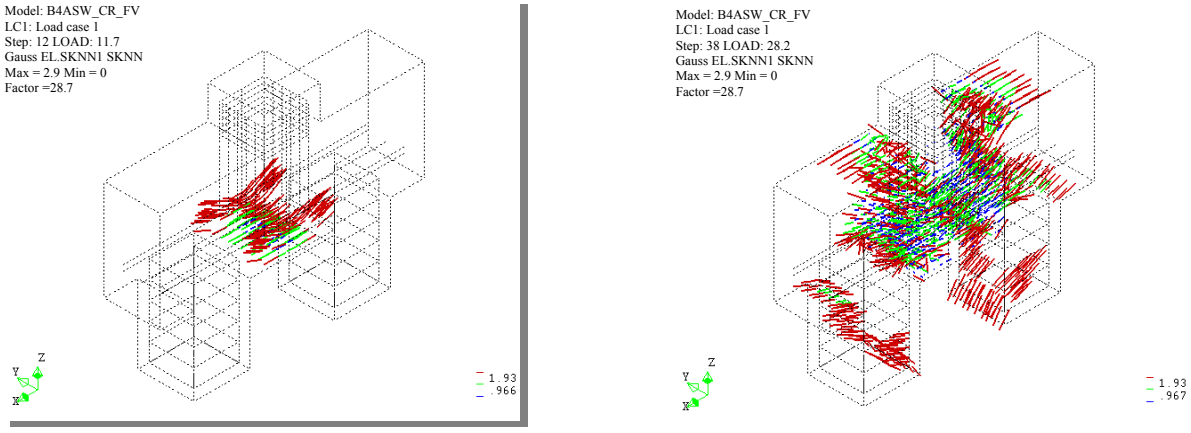

Figure 12. Compression stress flow on model BLH75A55_20.

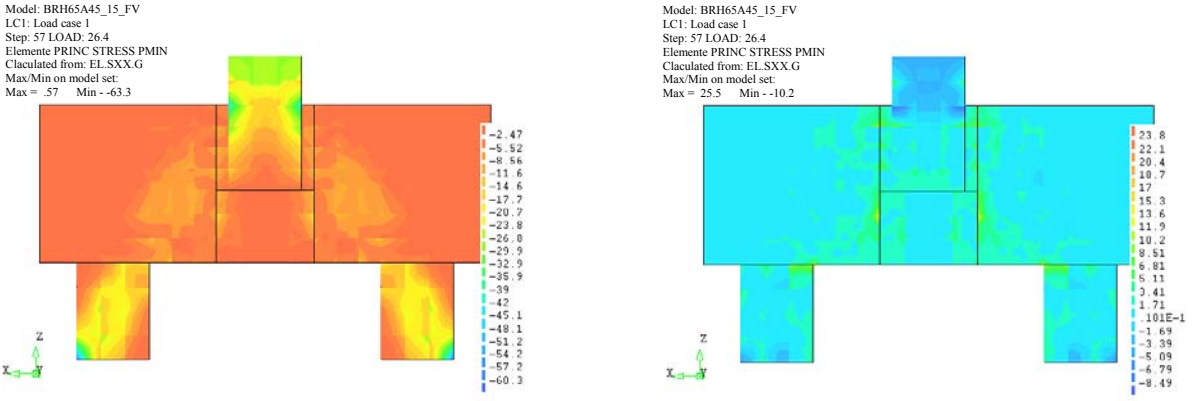

Figure 13. Principal compression and tensile stress flow on the model BLH75A55_20.

Table 6. Ultimate load in Column and failure mode.

Model	Ultimate Load (kN)	Collapse	Failure mode	MODEL	Ultimate Load (kN)	Collapse	Failure mode
BLH75A45_15	2429	Reinf.	fragile	BRH65A45_15	2377,8	Conc.	fragile
BLH75A45_15_cv1	2458,8	Reinf.	fragile	BRH65A45_15_cv1	2376,8	Conc.	fragile
BLH75A45_15_cv2	2495,7	Reinf.	fragile	BRH65A45_15_cv2	2430	Conc.	fragile
BLH75A45_20	2253,6	Reinf.	ductile	BRH65A45_20	2298	Reinf.	ductile
BLH75A45_20_cv1	2347,2	Conc.	ductile	BRH65A45_20_cv1	2394	Reinf.	ductile
BLH75A45_20_cv2	2357,1	Reinf.	ductile	BRH65A45_20_cv2	2302	Reinf.	ductile
BLH75A55_15	2880	Conc.	fragile	BRH65A55_15	3298	Conc.	fragile
BLH75A55_15_cv1	2892,6	Conc.	fragile	BRH65A55_15_cv1	3033	Conc.	fragile
BLH75A55_15_cv2	2495,7	Conc.	fragile	BRH65A55_15_cv2	3082	Conc.	fragile
BLH75A55_20	2396,7	Reinf.	ductile	BRH65A55_20	2858	Conc.	ductile
BLH75A55_20_cv1	2370,6	Reinf.	ductile	BRH65A55_20_cv1	2155	Conc.	ductile
BLH75A55_20_cv2	2298,6	Reinf.	ductile	BRH65A55_20_cv2	2101	Reinf.	ductile

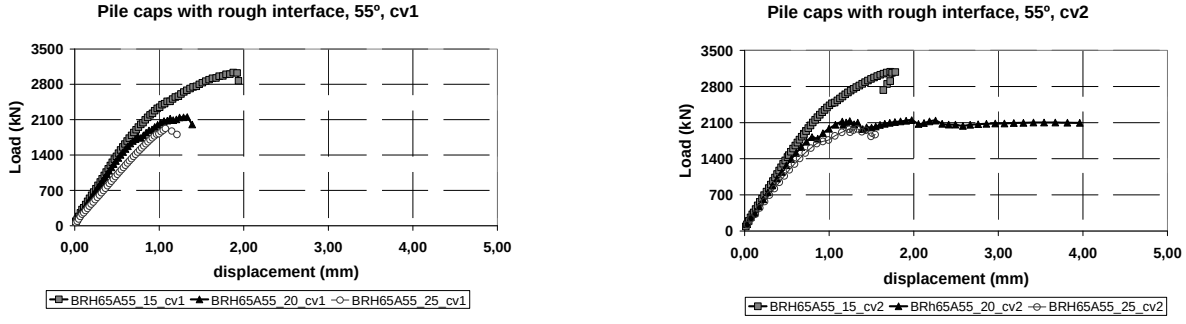

Figure 14. Influence of wall thickness on pile caps with rough interface, θ=55º.

Conclusion

In general, it was found that the presence of the locking beam in pile caps with embedded socket did not change the behavior of pile caps.

In relation to the wall thickness of the socket, for each group analyzed, models with wall thickness of 0.15 m presented the ultimate load greater than models whose wall thickness was equal to 0.20 m. This result was consistent independent of the strut angle value, interface type of socket walls and the presence or absence of locking beam. One factor that may have contributed to this result is that, pile caps with 0.20 m thick walls presents on the y direction, a distance between the face of the pile and limit of the pile cap greater than the recommended value of design criteria, which is half of the side of the pile.

Acknowledgements

Authors thank the Department of Structural Engineering of São Carlos Engineering School, University of São Paulo, CAPES and CNPq for the PhD scholarship to the first author.

References

ABNT-Associação Brasileira de Normas Técnicas. **NBR 9062**: Projeto e execução de estruturas de concreto pré-moldado. Rio de Janeiro: ABNT, 2006.

ABNT-Associação Brasileira de Normas Técnicas. **NBR 6118**: Projeto de Estruturas de concreto - Procedimentos. Rio de Janeiro: ABNT, 2007a.

ABNT-Associação Brasileira de Normas Técnicas. **NBR 7480**: Aço destinado a armaduras para estruturas de concreto armado - Especificação. Rio de Janeiro: ABNT, 2007b.

ASCE-American Society of Civil Engineers. ASCE-ACI COMMITTEE 445. Recent approaches to shear design of structural concrete. **Journal of Strucutral Engineering**, v. 124, n. 12, p. 1375-1417, 2009.

BANGASH, M. Y. H. **Manual of numerical methods in concrete**: modeling and applications by experimental and site-monitoring data. London: Thomas Telford Ltd., 2001.

BLÉVOT, J.; FRÉMY, R. Semelles sur piex. **Analles d'Institut Techique du Bâtiment et des Travaux Publics**, v. 20, n. 230, 1967, p. 223-295, 1967.

CANHA, R. M. F.; EL DEBS, M. K.; JAGUARIBE JUNIOR, K. B.; EL DEBS, A. L. H. C. Behavior of socket base connections emphasizing on pedestal walls. **ACI Structural Journal**, v. 106, n. 3, p. 268-278, 2009.

CHEN, W. F. **Plasticity in reinforced concrete**. New York: McGraqw-Hill Book Company, 1982.

DELALIBERA, R. G.; GIONGO, J. S. Influence of column cross section and eccentricity of compression load in structural behavior of two pile cap. **IBRACON Structure and Materials Journal**, v. 2, n. 4, p. 306-315, 2009.

DIANA. **Finite element analysis**. Element library. Delft: TNO DIANA, 2005.

KWAK, H. G.; NOH, S. H. Determination of strut-and-tie models using evolutionary structural optimization. **Engineering Structures**, v. 28, n. 10, p. 1440-1449, 2006.

LEONHARDT, F.; MÖNNIG, E. **Construções de concreto**. Rio de Janeiro: Interciência, 1978. v. 1-4.

NORI, V. V.; THARVAL, M. Design of pile caps. Strut-and-tie model method. **The Indian Concrete Journal**, **Point of view**, v. 51, n. 4, p. 13-19, 2007.

SCHLAICH, J.; SCHÄFER, K. Design and detailing of structural concrete using strut-and-tie models. **The Structural Engineer**, v. 69, n. 6, p. 113-125, 1991.

SOUZA, R. A.; KUCHMA, D. A.; PARK, J.; BITTENCOURT, T. N. Nonlinear finite element analysis of four-pile caps supporting columns subjected to generic loading. **Computers and Concrete**, v. 4, n. 5, p. 363-376, 2007.

SOUZA, R. A.; KUCHMA, D. A.; PARK, J.; BITTENCOURT, T. N. Adaptable strut-and-tie model for the design and verification of four pile caps. **ACI Structural Journal**, v. 106, n. 2, p. 142-150, 2009.

Received on November 26, 2012.
Accepted on June 19, 2013.